Polymer 51 (2010) 3715–3721

Contents lists available at ScienceDirect

Polymer

journal homepage: www.elsevier.com/locate/polymer

Facile fabrication of polystyrene/carbon nanotube composite nanospheres with core-shell structure via self-assembly

Chao Zhang [a], Tianxi Liu [a,*], Xuehong Lu [b,*]

[a] Key Laboratory of Molecular Engineering of Polymers of Ministry of Education, Department of Macromolecular Science, Laboratory of Advanced Materials, Fudan University, Shanghai 200433, PR China
[b] School of Materials Science and Engineering, Nanyang Technological University, 50 Nanyang Avenue, Singapore 639798, Republic of Singapore

ARTICLE INFO

Article history:
Received 27 January 2010
Received in revised form
5 June 2010
Accepted 10 June 2010
Available online 18 June 2010

Keywords:
Carbon nanotube
Polystyrene nanospheres
Hydrogen-bonding self-assembly

ABSTRACT

In this paper, a novel method for fabrication of core-shell nanospheres with polystyrene (PS) as the core and multi-walled carbon nanotubes (MWNTs) as the shell via hydrogen-bonding self-assembly is introduced. The PS nanospheres with carboxyl acid groups on the surface (PS–COOH nanospheres) were prepared by typical soap-free emulsion copolymerization with acrylic acid as comonomer. The MWNTs were grafted with poly(vinyl pyrrolidone) (PVP), in which the carbonyl oxygen can act as proton acceptors to form hydrogen bonds with the carboxyl acid groups. The results show that the functionalized MWNTs can self-assemble onto the surface of PS–COOH nanospheres rapidly via hydrogen bonding interaction, and the process is reversible and can be well controlled by adjusting pH value of the system. These core-shell nanospheres have the potential to be used as conductive and synergistic reinforcement fillers in fabricating high-performance and functional nanocomposites.

1. Introduction

Since the discovery of carbon nanotubes (CNTs) in 1991, because of their unique structure and outstanding properties, great interest has been aroused in areas such as fabrication, characterization and applications of CNTs. Pristine CNTs cannot be dissolved and manipulated in almost any solvent, and they are also difficult to be dispersed well in solid matrices, which greatly limit their applications in many fields. Progress in the development of functionalization methods and novel self-assembly techniques for CNTs has widened their application range in recent years [1–4]. In particular, polymers have been utilized for functionalizing CNTs through either wrapping or covalent bonding, which has enabled the dispersion of CNTs into aqueous and organic liquid media as well as polymer matrices and opened up new possibilities of developing novel structures and materials. Among various covalent functionalization methods for CNTs, defect functionalization is a simple but effective method, and has become the subject of intensive investigations for fabricating novel materials with new functions and applications [5,6].

Construction of core-shell super-structures with CNTs as the shell has attracted much attention because of their potential applications in chromatography techniques, nanoscale electronic devices, etc. CNTs have been assembled on various types of colloidal templates using the well-known layer-by-layer (LBL) assembly technique based on electrostatic interaction [7–13] and van der Waals attractions [14]. Although the LBL assembly is an effective technique to deposit dense mono- and multi-layers of CNTs onto colloidal templates, the processes are intricate and tedious. A simpler approach to prepare core-shell polymer/CNT spheres is to use surfactants to stabilize CNTs and then mix the well-dispersed CNTs with polystyrene (PS) or poly(methyl methacrylate) (PMMA) microspheres to induce slow sedimentation of the two components, finally forming the CNT-adsorbed polymer microspheres [15]. However, using this method, the residual surfactants are difficult to be removed, which may largely affect the properties of the prepared particles and their further uses. Recently, some researchers have attempted to prepare CNT hollow spheres by simple emulsion method [16–19]. Enrichment of CNTs in the interface between water and oil phases was utilized in these studies. As only the liquid phase is used as the core, the as-prepared hollow CNT particles are of irregular shape, and the size is usually larger than 5 μm, sometimes even up to 10–100 μm with a very wide size-distribution, thus limiting their further applications.

In this paper, we report a facile approach to fabrication of PS-CNT core-shell nanoparticles by simply mixing aqueous dispersions of poly(*N*-vinylpyrrolidone) (PVP)-grafted MWNTs obtained via defect functionalization and acid-functionalized PS (PS–COOH)

* Corresponding authors. Tel.: +86 21 55664197; fax: +86 21 65640293.
E-mail addresses: txliu@fudan.edu.cn (T. Liu), asxhlu@ntu.edu.sg (X. Lu).

0032-3861/$ – see front matter © 2010 Elsevier Ltd. All rights reserved.
doi:10.1016/j.polymer.2010.06.021

nanospheres. The motivation of the work is to fabricate nanohybrid structures consisting of 1-D nanoparticles (CNTs) and 3-D nanoparticles (polymer nanospheres) in a simple but controllable way. Co-assembly of mixed nanoparticles with different sizes and shapes opens up the possibility of fundamentally studying assembly behavior of two kinds of nanomaterials [20–22]. The self-assembly tendency of PVP-functionalized MWNTs and PS–COOH nanospheres can be controlled by varying pH values of the solutions, which promises easy manipulation of morphology of the core-shell nanoparticles. The reverse process, i.e. the dissociation of the aggregated composite nanoparticles, is also made possible, which is important to study the resultant nanoaggregates with electronic, optical, magnetic and biological properties derived from the two individual nanomaterials.

2. Experimental

2.1. Materials

Styrene, *N*-vinyl pyrrolidone (NVP) and acrylic acid, supplied by Sigma–Aldrich, were purified by distillation under reduced pressure. Allyl glycerol ether (AGE), concentrated nitric acid (69%), concentrated hydrochloric acid (36.5%), *N,N*-dimethylformamide (DMF) and acetone were supplied by Sigma–Aldrich and used as received. Potassium persulfate (KPS) and 2,2′-azobisisobutyronitrile (AIBN) were purchased from Sigma–Aldrich and used after recrystallization. MWNTs with purity of 95%, produced by CVD method, were supplied by Chengdu Institute of Organic Chemistry, Chinese Academy of Sciences. The outer diameters of the MWNTs are about 10–20 nm. Ultrapure Milli-Q water was used throughout all the experiments.

2.2. Measurements and characterization

FTIR spectra were recorded with a spectral resolution of 4 cm^{-1} on a Nicolet Nexus 470 spectrometer equipped with a DTGS detector by signal averaging of 256 scans. IR samples were in the form of KBr pellets containing 1 wt% pre-dried sample. Thermogravimetric analysis (TGA) was performed from 100 to 800 °C at a heating rate of 10 °C/min using Q-500 (TA Instruments) under nitrogen atmosphere. The digital images were taken by Canon Digital IXUS 80IS. TEM samples were prepared by dispersing the CNTs in ethanol through sonication and casting the suspensions onto Cu grids, followed by solvent evaporation in air at room temperature. The surface morphology of the nanospheres was observed by a JEOL JSM-6700 field emission scanning electron microscope (FESEM) under an accelerated voltage of 5.0 kV.

2.3. Preparation of PS–COOH nanospheres via soap-free emulsion polymerization

PS–COOH nanospheres with styrene/acrylic acid molar ratio of 9:1 were synthesized as previously reported [23–25]. The soap-free emulsion polymerizations were carried out in a 250 mL three-neck flask equipped with a reflux condenser, nitrogen gas inlet, Teflon stirrer, and thermometer. The targeted solid content of the emulsion was 10 wt% and the initial charge in the reactor was deionized water, styrene and acrylic acid. After pre-emulsification for 30 min, the glass reactor was degassed with nitrogen for 30 min at 70 °C. The initiator solution was then added slowly, followed by polymerization at 70 °C for 6 h. After the emulsion was cooled down to room temperature, the products were washed several times with methanol by centrifuging and then dried under vacuum at 35 °C for 24 h.

2.4. Acid treatment of the raw MWNTs

In a typical experiment, 1 g raw MWNTs were added into a 250 mL round-bottom flask, with 100 mL 69% nitric acid. The mixture was sonicated (with a frequency of 40 Hz) for 10 min and then heated to reflux (at 90 °C) for 24 h. After cooling to room temperature, the mixture was diluted with 800 mL deionized water and then filtered with filter paper. The black solid on the paper was then redispersed in water and filtered with 0.45 μm Milipore PTFE membrane. The dispersing and filtration steps were repeated at least four cycles, until the pH value of the filtrate approached 7. The final black solid was collected by centrifuging and then dried under vacuum for 24 h at 60 °C.

2.5. Preparation of PVP-PAGE random copolymer and PVP-functionalized MWNTs

PVP-PAGE random copolymer was prepared by typical radical copolymerization using AIBN as radical initiator and DMF as solvent. The flask was tightly sealed with a rubber septum and then degassed. The polymerization was conducted at 70 °C with NVP/AGE of 20:1 in an oil bath. After 12 h, the acid-treated MWNTs dispersed in DMF were injected into the upper reaction solution. The solution was kept at 120 °C and catalyzed by 1 wt% TEA for 24 h. The product was then collected by centrifuging and washed several times by filtration with large amount of water, ethanol and dried under vacuum overnight.

2.6. Fabrication of PS/CNT core-shell nanospheres

A homogeneous dispersion of PVP-g-MWNTs in water with the concentration of 1.0 mg/mL (Suspension I) and an aqueous suspension of 1 wt% PS–COOH (Suspension II) were prepared by sonication and adjusted to pH = 3 by adding 1.0 mol/L HCl. Both suspensions were found stable after at least one day storage. 1 mL Suspension II was dropped into 5 mL Suspension I in 2 min under vigorous stirring. After that, the mixture was kept at ambient condition for at least 5 min without stirring. Gradually, gray black precipitates were found at the bottom of the bottle and the upper solution became clear and transparent. After centrifugation and washing with water, the precipitates were dried under vacuum overnight for further characterization. When these gray black precipitates were added into deionized water that was adjusted to pH = 10 by adding NaOH solution, they were redispersed into solutions. Samples with different concentrations of PVP-g-MWNTs (0.20 mg/mL and 0.04 mg/mL) were fabricated by repeating the above experimental procedure.

3. Results and discussion

In this work, the method used for adsorbing MWNTs onto spherical colloids is based on the typical hydrogen-bonding-induced self-assembly of poly(acrylic acid) (PAA) and PVP, which is similar to the LBL self-assembly of PAA and PVP reported by other groups [26–28]. However, since PAA is completely water soluble and cannot form nanospheres in water, we introduce large amount of carboxyl acid groups onto the surface of PS nanospheres via a one-step soap-free emulsion copolymerization process. The particle size, copolymer composition, and surface groups of the nanospheres can be tailored and the PAA phase can be enriched on the surface of the latex [29,30].

The MWNTs were functionalized in two steps as illustrated in Fig. 1. In the first step, the MWNTs were functionalized by acid treatment, whereby carboxyl acid and hydroxyl groups were introduced onto their end tops and side walls. In the second step,

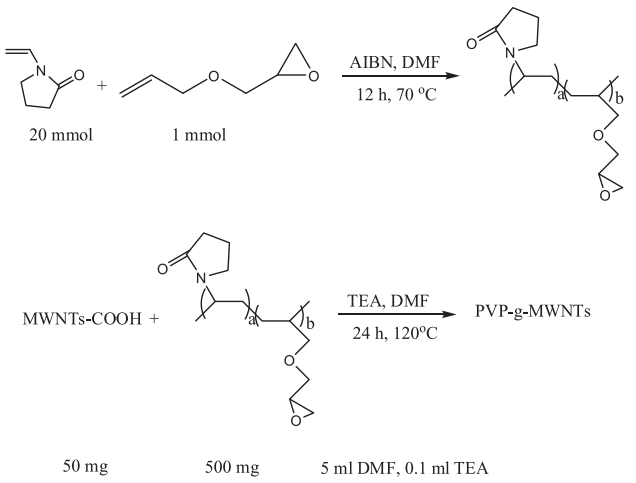

Fig. 1. Schematic illustration of the functionalization of MWNTs.

the PVP-PAGE copolymer was grafted onto the surface of the acid-treated MWNTs by simple epoxy ring-opening reaction.

Fig. 2 shows the FTIR spectra of the raw MWNTs, the acid-treated MWNTs (MWNT-COOH) and the PVP-grafted MWNTs (PVP-g-MWNTs). Compared with the raw MWNTs (curve *a*), the FTIR spectrum of MWNT-COOH (curve *b*) shows an absorption band at 1738 cm^{-1} that can be assigned to carbonyl stretching vibration, indicating that the carboxyl acid groups have been introduced onto the MWNT backbones after oxidization by concentrated HNO_3. Curve *c* in Fig. 2 shows the FTIR spectrum of PVP-g-MWNTs. Different from that of MWNT-COOH, distinct signals from PVP can be seen clearly on the curve *c*. The broad bands in the wavenumber range of 3000–3500 cm^{-1} are related to the trace amount of residual water in KBr used for preparation of the samples, whereas the C–H stretching vibrations of the grafted PVP and PAGE can be observed at 2860 and 2930 cm^{-1}. The broad absorption band at 1650 cm^{-1} corresponds to the stretching vibration of the C=O group of the amide. The broad but relatively weak band at 1430 cm^{-1} is assigned to the stretching vibration of the C–N bond of the amide group. No bands corresponding to epoxy rings are detected, indicating that the epoxy ring-opening reaction does occur. The FTIR results thus verify that PVP chains are covalently attached to the MWNTs.

In order to estimate the weight percentage of carboxyl acid and hydroxyl groups upon acid treatment and that of PVP chains grafted onto the MWNTs, functional groups and grafted polymer chains on the MWNTs were removed by thermal defunctionalization. Fig. 3 presents the weight loss curves of the MWNT samples upon heating in a nitrogen atmosphere. As shown in Fig. 3, only about 1.8 wt% weight loss, mainly contributed by the decomposition of amorphous carbon or the residual metal catalysts, can be observed for the raw MWNTs when the temperature is increased to 600 °C, indicating a good thermal stability of the raw MWNTs. In contrast, the MWNT-COOH sample starts to lose weight at about 150 °C as a result of the decomposition of the functional groups, i.e. carboxyl acid and hydroxyl groups, on the MWNTs. According to the residual weight at 600 °C, the amount of the functional groups is estimated to be about 5.0 wt% in the MWNT-COOH sample. This value is comparable to the results reported previously [31,32]. Similarly, the amount of PVP chains in PVP-g-MWNTs is estimated to be about 18.2 wt%. Clearly, the MWNTs are successfully functionalized with PVP by the two-step process.

As shown in Fig. 4, the raw MWNTs cannot be dissolved in any solvents studied, such as deionized water and DMF. After the acid treatment, the resulting MWNT-COOH can only be poorly dispersed in water, whereas it exhibits good solubility in DMF. In contrast, a very good solubility of PVP-g-MWNTs can be observed in solvents such as water and DMF, which is almost similar to the solubility behavior of neat PVP. However, PVP-g-MWNTs exhibit poor solubility in acetone, just as neat PVP does, confirming that the PVP chains have indeed been covalently bonded to the MWNTs.

The TEM images of the raw MWNTs and PVP-g-MWNTs are shown in Fig. 5. The internal and external diameters of the raw nanotubes are about 5–10 and 10–20 nm, respectively. The average length of the MWNT is approximately several micrometers. For the images of the raw MWNTs, no extra phase marked with different degrees of gray can be observed in the images at low and high magnifications (Fig. 5a, b). For the samples of PVP-g-MWNTs, in the low magnification image (Fig. 5c), it can be seen that some parts of the tubes are clothed with a polymer layer, and the jointed tubes still mass together. This indicates that the thickness of the polymer

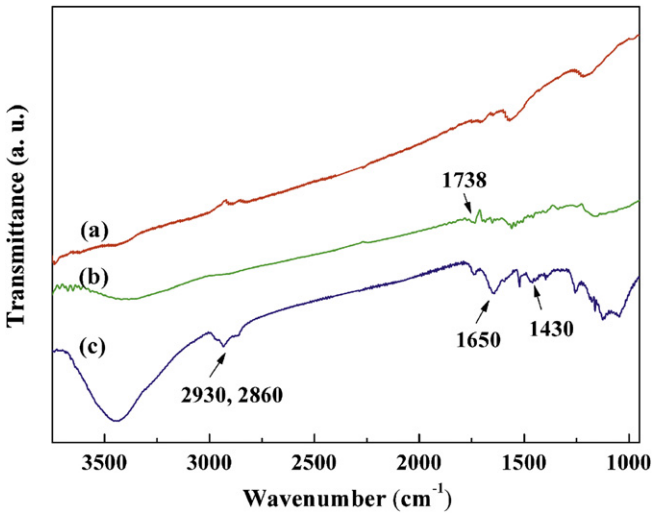

Fig. 2. FTIR spectra of (a) the raw MWNTs, (b) MWNTs-COOH and (c) PVP-g-MWNT samples.

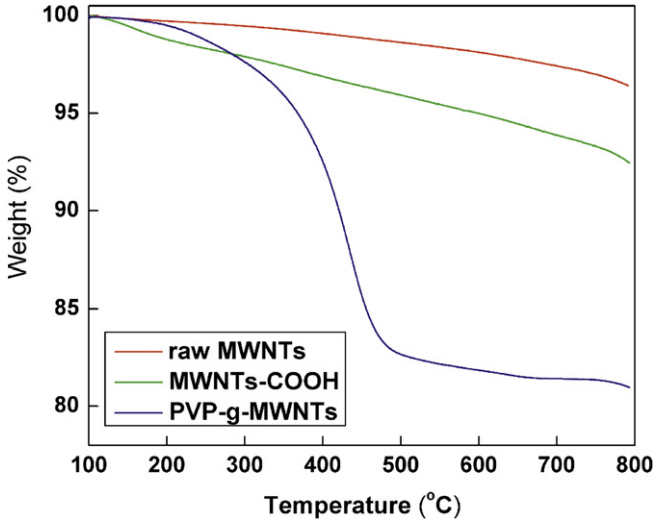

Fig. 3. Temperature dependence of weight loss for the raw MWNTs, MWNT-COOH and PVP-g-MWNTs in nitrogen flow.

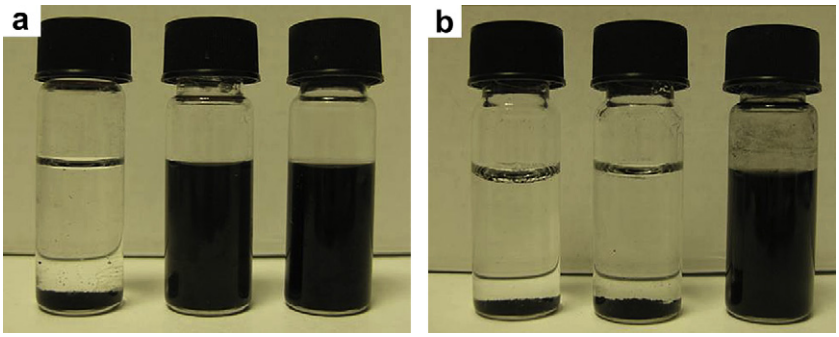

Fig. 4. The dispersion state of the raw MWNTs (left), MWNT-COOH (middle) and PVP-g-MWNTs (right) in (a) distilled water and (b) DMF. The photos were taken after 1 month storage. The content of CNTs in each bottle is 1.0 mg/mL.

layer coated on the MWNT is not completely same and the "grafting onto" process occurs not only at the tube tips but also on the whole convex surfaces. In the images at high magnification (Fig. 5d), the core-shell structure is clearly observed. The polymer layer is closely impinged on the outer wall along the stretched direction of the nanotubes. The thicknesses of polymer layer grafting on MWNTs are measured to be about 2–4 nm. These observations are in agreement with those ever reported for other polymer-functionalized MWNTs, wherein similar core-shell structure was formed when certain amount of polymer was grafted onto MWNTs.

When the concentration of PS–COOH nanospheres in the colloidal suspension of PS–COOH is 1wt% and the concentrations of PVP-g-MWNTs in water are 1.0, 0.20, 0.04 and 0 mg/mL, respectively, all suspensions are fairly stable at pH = 3 after standing for one day, as shown in Fig. 6a. When the colloidal suspension of PS–COOH nanospheres is dropped into the aqueous dispersions of PVP-g-MWNTs, interestingly, PVP-g-MWNTs can be adsorbed onto the surfaces of the PS–COOH nanospheres rapidly, thereby inducing co-precipitation of the composite nanospheres. As a result, fast sedimentation occurs, as shown in Fig. 6b, indicating the presence of strong interactions between PS–COOH nanospheres and PVP-g-MWNTs. Even after sonicating these sediments in deionized water for several minutes, the MWNTs still remain adhered to the surfaces of PS–COOH nanospheres due to the strong hydrogen bonding interaction between the two components. When adjusting the upper clear, transparent solvent into alkaline condition (pH = 10) and stirring gently, the gray black precipitates at the bottom of the bottle can be redispersed into the upper clear solvent homogeneously, as shown in Fig. 6c, indicating the elimination of the hydrogen bonding interaction due to the ionization of carboxyl acid group under the alkaline condition.

Fig. 7 presents the thermal degradation behaviors of PS–COOH nanospheres, PVP-g-MWNTs and the composite nanospheres prepared at the PVP-g-MWNTs loading of 1.0 mg/mL. PS–COOH nanospheres show a two-stage decomposition. The first stage is in the temperature region of 200–350 °C, which is probably related to the cleavage of surface carboxyl acid groups in PS–COOH nanospheres. The second one starts at about 350 °C, which is assigned to the decomposition of PS chains in the core. The PS/MWNT composite nanospheres show thermal decomposition in the temperature range of 250–500 °C and a weight loss of about 78%. The residues above 500 °C are mainly the MWNTs left behind

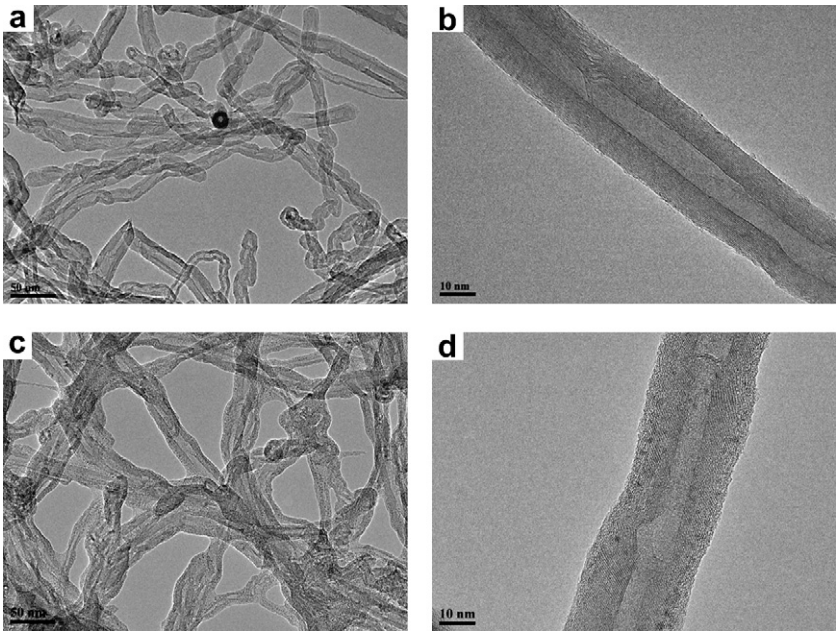

Fig. 5. TEM images of the raw MWNTs at low (a) and high (b) magnifications; the PVP-g-MWNTs at low (c) and high (d) magnifications.

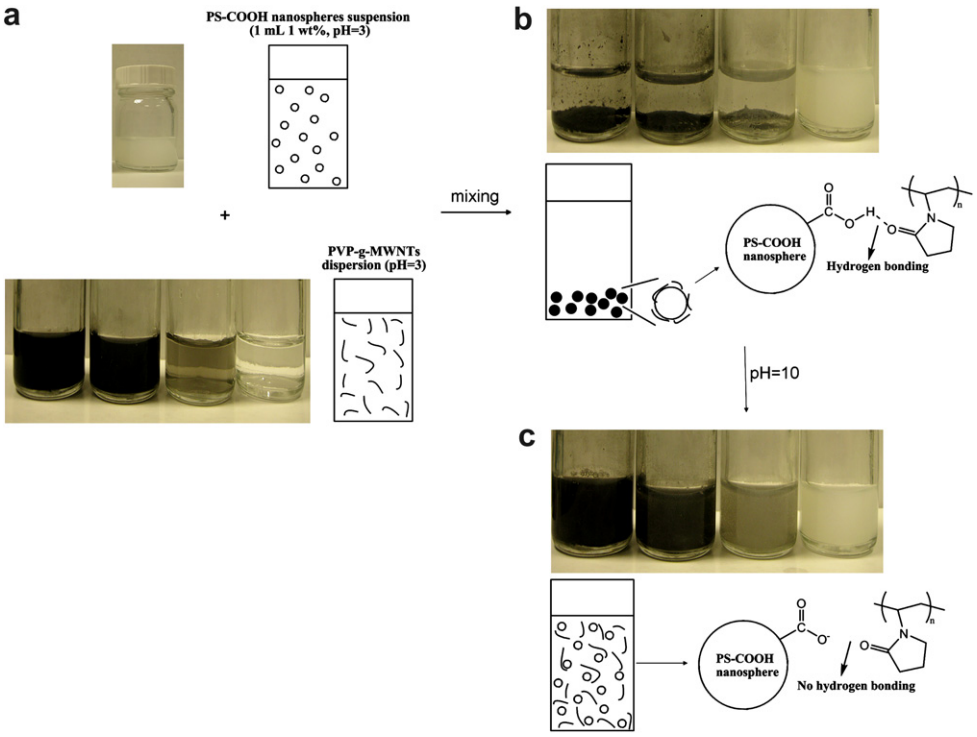

Fig. 6. Schemes showing the fabrication process of the PS/MWNT core-shell composite nanospheres and the dissociation process of the aggregated composite particles. (a) PS–COOH colloidal suspension with a concentration of 1 wt% and PVP-g-MWNT suspensions in water with concentrations of 1.0, 0.20, 0.04 and 0 mg/mL, respectively. All the suspensions were adjusted to pH = 3; (b) co-precipitation of PS–COOH colloidal suspension and PVP-g-MWNT suspensions with concentrations of 1.0, 0.20, 0.04 and 0 mg/mL, respectively; (c) dissociation of the aggregated composite particles via varying pH to 10.

without organic groups, indicating that a significant amount of MWNTs have been adsorbed onto PS–COOH nanospheres. It is worth noting that the contents of MWNTs in the core-shell composite nanospheres can be controlled conveniently by changing the initial weight ratio of PVP-g-MWNTs to PS–COOH nanospheres in the solutions. In the LBL assembly process, this is usually done by changing the cycle numbers, which is more tedious and time-consuming.

Direct evidence for the adsorption of PVP-g-MWNTs on the surface of PS–COOH nanospheres can be obtained by FESEM observation. Fig. 8 shows the surface morphologies of the as-prepared PS–COOH nanosphere and PS/MWNTs composite nanospheres with different loadings of PVP-g-MWNTs. Fig. 8a is the FESEM image at a low magnification for the PS–COOH nanospheres produced by emulsion technology without any treatment. These nanoparticles have a narrow size-distribution and average particle size of ~280 nm. The image at a higher magnification (Fig. 8b) shows relatively clean surface with some bitty gullies for the as-prepared PS–COOH nanospheres. Fig. 8c, d and e show the morphologies of the PS/MWNT core-shell nanospheres with different loading levels of PVP-g-MWNTs (0.04, 0.20, 1.0 mg/mL, respectively). From these FESEM images, it can be observed that the amount of the MWNTs adsorbed on the surface of PS–COOH nanospheres increases with the initial loading levels of PVP-g-MWNTs. The uncovered region of the core-shell nanosphere surface is clean and smooth, while the rough region with tiny hair-like structures corresponds to the MWNTs adsorbed on the nanosphere surface. At high MWNT loading levels, some MWNTs form joints between PS–COOH nanospheres. The above FESEM images further confirm that each colloidal particle of PS–COOH has MWNTs adsorbed on the surface, while MWNTs or PS nanospheres themselves do not aggregate forming large agglomerates. Fig. 8f shows the same sample as in Fig. 8e but at a higher magnification. One can clearly see the hair-like structures of CNTs on the smooth surface of PS–COOH nanospheres. To further study the formation mechanism of these PS/MWNT nanospheres, they were put into alkaline condition (pH = 10) to destroy the hydrogen bonding interaction. After the alkaline treatment, the MWNTs are seldom observed on the surface of PS–COOH nanospheres, as clearly shown in Fig. 8 g. This verifies that the MWNTs are indeed adsorbed onto the surface of the PS–COOH nanospheres through hydrogen bonding interaction.

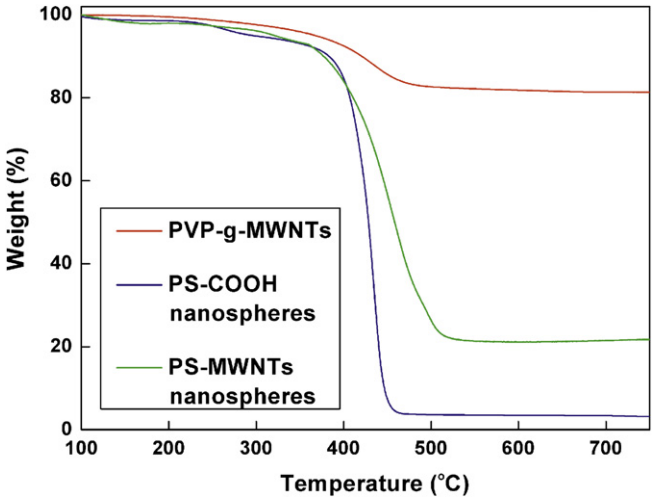

Fig. 7. Temperature dependence of weight loss for PVP-g-MWNTs, PS–COOH nanospheres and PS-MWNT core-shell nanospheres in nitrogen flow.

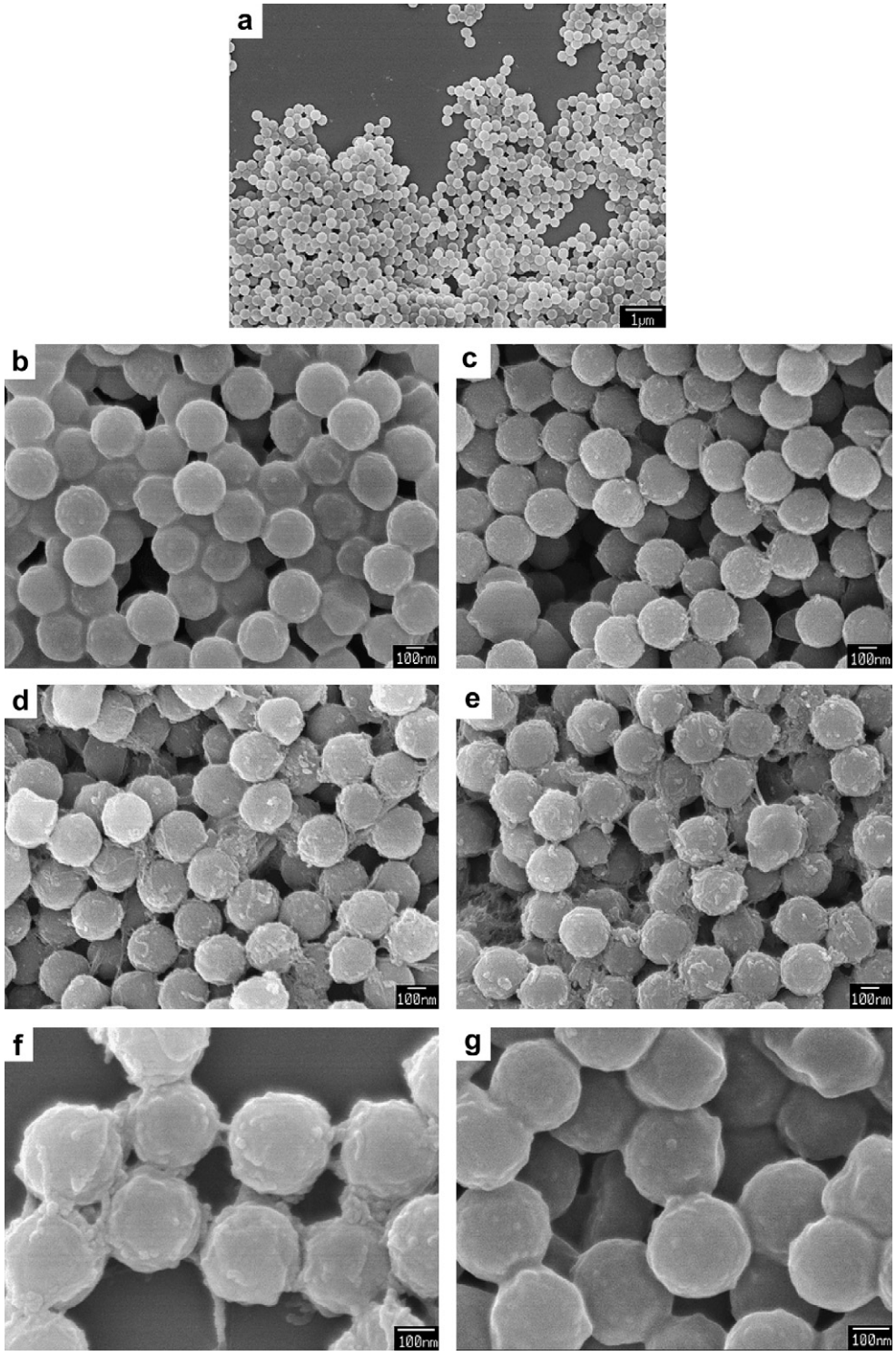

Fig. 8. FESEM images of the as-prepared PS–COOH nanospheres at low (a) and high (b) magnifications, PS/MWNT core-shell nanospheres with PVP-g-MWNT loadings of 0.04 mg/mL (c), 0.20 mg/mL (d) and 1.0 mg/mL (e), respectively, at pH = 3. (f) is a high-magnification FESEM image of PS/MWNT core-shell nanospheres at PVP-g-MWNT loading of 1.0 mg/mL and pH = 3; (g) shows that after adjusting pH value to 10 and rinsing, the surface of the nanospheres shown in (f) becomes clean and smooth.

4. Conclusions

In summary, the present paper demonstrates that polystyrene/MWNT composite nanospheres with well-controlled morphology can be obtained at large scale by a facile wet chemical self-assembly method. The loading level of MWNTs within the hybrid nanospheres can be easily controlled by changing the initial proportion of MWNT and PS–COOH nanospheres. MWNTs are observed on the surface of nanospheres with a small amount of MWNT joints among the spheres. The hydrogen-bonding self-assembly process is reversible and can be well controlled by adjusting pH value of the system. The hybrid nanoparticles prepared via this route have the potential to be used as conductive and synergistic reinforcement fillers for fabricating high-performance and functional nanocomposites. Detailed

studies are still on the way to investigate the properties and applications of these nanoaggregates.

Acknowledgments

C.Z. and T.L. thank the School of Materials Science and Engineering, Nanyang Technological University (NTU), for financial support through a Visiting Scientist Program. T.L. gratefully acknowledges the financial support from the National Natural Science Foundation of China (20774019, 50873027), "Shu Guang" project supported by Shanghai Municipal Education Commission and Shanghai Education Development Foundation, and the Shanghai Leading Academic Discipline Project (Project Number: B113).

References

[1] Liu J, Rinzler AG, Dai H, Hafner JH, Bradley RK, Boul PJ, et al. Science 1998;280(5367):1253–6.
[2] Nguyen CV, Delzeit L, Cassell AM, Li J, Han J, Meyyappan M. Nano Lett 2002;2(10):1079–81.
[3] Stevens JL, Huang AY, Peng H, Chian IW, Khabashesku VN, Margrave JL. Nano Lett 2003;3(3):331–6.
[4] Dyke CA, Tour JM. J Am Chem Soc 2003;125(5):1156–7.
[5] Qi P, Vermesh O, Grecu M, Javey A, Wang Q, Dai H, et al. Nano Lett 2003;3(3):347–51.
[6] Wong SS, Joselevich E, Woolley AT, Cheung CL, Lieber CM. Nature 1998;394(6688):52–5.
[7] Correa-Duarte M, Kosiorek A, Kandulski W, Giersig M, Salgueirino-Maceira V. Small 2006;2(2):220–4.
[8] Paunov VN, Panhuis M. Nanotechnology 2005;16(9):1522–5.
[9] Menna E, Negra FD, Prato M, Tagmatarchis N, Ciogli A, Gasparrini F, et al. Carbon 2006;44(8):1609–13.
[10] Correa-Duarte M, Kosiorek A, Kandulski W, Giersig M, Liz-Marzan LM. Chem Mater 2005;17(12):3268–72.
[11] Huang XJ, Li Y, Im HS, Yarimaga O, Kim JH, Jang DY, et al. Nanotechnology 2006;17(12):2988–93.
[12] Shi J, Chen Z, Qin Y, Guo Z. J Phys Chem C 2008;112(31):11617–22.
[13] Tang M, Qin Y, Wang Y, Guo Z. J Phys Chem C 2009;113(5):1666–71.
[14] Sano M, Kamino A, Okamura J, Shinkai S. Nano Lett 2002;2(5):531–3.
[15] Jin HJ, Choi HJ, Yoon SH, Myung SJ, Shim SE. Chem Mater 2009;17(16):4043–7.
[16] Panhuis M, Paunov VN. Chem Commun 2005;13:1726–8.
[17] Ji L, Ma J, Zhao C, Wei W, Ji L, Wang X, et al. Chem Commun 2006;11:1206–8.
[18] Yi H, Song H, Chen X. Langmuir 2007;23(6):3199–204.
[19] Su J, Fu SJ, Gwo S, Lim KJ. Chem Commun 2008;43:5631–2.
[20] Daniel MC, Astruc D. Chem Rev 2004;104(1):293–346.
[21] Templeton AC, Wuelfing WP, Murray RW. Acc Chem Res 2000;33(1):27–36.
[22] Niemeye CM. Angew Chem Int Ed 2001;40(22):4128–58.
[23] Kang K, Kan CY, Du Y, Liu DS. J Appl Polym Sci 2004;92(1):433–8.
[24] Yan LF, Zhang GZ, Liu GM, Ji J, Li W. J Appl Polym Sci 2006;100(5):3718–26.
[25] Xu SY, Han XZ. Biosens Bioelectron 2004;19(9):1117–20.
[26] Ishiduki K, Esumi K. Langmuir 1997;13(6):1587–91.
[27] Tian Y, He Q, Cui Y, Tao C, Li JB. Chem Eur J 2006;12(18):4808–12.
[28] Fu Y, Bai SL, Cui SX, Qiu DL, Wang ZQ, Zhang X. Macromolecules 2002;35(25):9451–8.
[29] Fulda KU, Kampes A, Krasemann L, Tieke B. Thin Solid Films 1998;327:752–7.
[30] Yan C, Cheng SY, Feng LX. J. Polym. Sci. Part A, Polym Chem 1999;37(14):2649–56.
[31] Tsang SC, Chen YK, Harris PJF, Green MLH. Nature 1994;372(7279):159–62.
[32] Sun YP, Fu K, Lin Y, Huang W. Acc Chem Res 2002;35(12):1096–104.